

Supporting Information

Strong, Tough and Anisotropic Bioinspired Hydrogels

Shu Wang^{a,b†}, Ling Lei^{a†}, Yuanhao Tian^c, Huiming Ning^{a*}, Ning Hu^{a,d*}, Peiyi Wu^c, Hanqing Jiang^f,
Lidan Zhang^g, Xiaolin Luo^h, Feng Liu^a, Rui Zou^d, Jie Wen^d, Xiaopeng Wu^a, Chenxing Xiang^a, Jie Liu^{i*}

Materials and methods

Materials

PVA was purchased from Macklin with a degree of polymerization (DP) of about 1700 and a saponification degree of 99%. Glycerol was supplied by Guangdong Guanghua Sci-Tech Co. Ltd. Methanol and NaCl were purchased from Aladdin.

Preparation of anisotropic fiber-based hydrogel

After purified by DI water and methanol, the purified PVA was dissolved in DI water and stirred at 95 °C for 2 h to obtain a 10 wt.% PVA solution. Then, the 10 wt.% PVA solution was injected at a rate of 0.05 ml min⁻¹ through a stainless steel needle (25 G) into a cold methanol coagulation bath maintained at a temperature between -10°C and -15°C for the coagulation into fibers.^{1,2} An electric rotating platform can rotate the coagulation bath at 7.5 rpm. The spun wet PVA fibers were directionally collected to a certain width on a rotating spool controlled by a variable-speed motor (Movie 1). After being thoroughly dried at room temperature in a vacuum oven at 60 °C, PVA fibers were immersed in PVA/glycerin aqueous solutions at different concentrations (Table S3) at 60°C for 12 h to fully swell. The swollen fibers were then sandwiched between two layers of polypropylene films and flattened, and the excess solution was removed. Finally, after three freeze-thaw cycles, the anisotropic fiber-based hydrogels were obtained. In order to enhance ionic conductivity, NaCl was incorporated into the impregnating solutions during the initial mixing processes of PVA, glycerol and DI water. The content of NaCl ranged from 0.25 wt.% to 1 wt.%.

Mechanical test

The mechanical properties of the hydrogels were characterized using a universal testing machine (Shimadzu, model EZ-LX, 500N, Japan) at room temperature. The tensile speed and gauge length for tensile measurements were 30 mm/min and 8 mm, respectively. The elastic modulus was calculated from the linear region ($\epsilon=0-25\%$) of the tensile stress-strain curves. The toughness of the hydrogels was calculated as the area under tensile stress-strain curves. Each type of the prepared hydrogel was measured 5 times to obtain the average value. A pure shear test was performed using the above tensile tester at 20 mm/min, following the method established in reference.³ Two samples, notched and unnotched, were used to measure the fracture energy Γ . The samples were cut into a rectangular shape with a width of 20 mm and a length of 30 mm (a_0). The sample thickness was 0.47 mm (b_0). An initial notch of 10 mm in length was cut and the distance between the two clamps was fixed at 8 mm (L_0). The force-length curves of the samples were recorded and the tearing energy was calculated from $\Gamma=U(L_c)/(a_0 \times b_0)$, where $U(L_c)$ is the work done by the applied force to the unnotched sample at the critical stretching displacement L_c of the moving clamp, where L_c is the displacement at which the crack growth initiates in the notched sample.

Electrical test

An impedance analyzer (TH2839) was used to test the conductivity of the anisotropic fiber-based hydrogels and PVA hydrogels. The conductivity (σ , S m⁻¹) was calculated by the following formula: $\sigma=L/(R \times S)$, where L is the distance between adjacent electrodes, and R and S are the resistance and cross-sectional area of the hydrogel, respectively. The change in resistance of the hydrogels after applying a strain was recorded by combining a digit multimeter (Keysight 34465A) and a universal testing machine. The relative resistance change rate was calculated by the following formula: $\Delta R/R_0=(R-R_0)/R_0 \times 100\%$, where R_0 and R are the resistance of the original hydrogel and stretching hydrogel, respectively. Moreover, the gauge factor (GF) indicating the sensitivity of the hydrogel was obtained by using the following formula: $GF=(\Delta R/R_0)/\epsilon$, where ϵ represents the applied strain.

Environmental stability test

The water retention capacity test was carried out by keeping the samples in an environmental chamber with a 50% relative humidity (RH) at 25 °C for 12 days. The anti-freezing performance of the hydrogel was analyzed by a differential scanning calorimetry (DSC, Netzsch DSC214). The temperature for testing ranged from -85°C to 25°C, and the heating rate was 10°C min⁻¹. The hydrogels were immersed in DI water for 72 h. During this period, the swelling properties were measured by wiping and weighing the water content on the surface of the hydrogel after the hydrogel was taken out at intervals from the DI water.

In vitro cytotoxicity test

The MTS assay was utilized to detect the cytotoxicity and compatibility of the hydrogels by the viability of L929 fibroblast cells that were incubated with hydrogel leaching media.⁴ The hydrogel leaching media were obtained by immersing the hydrogels in the dulbecco's modified eagle medium (DMEM) for 7 days. L929 fibroblasts were inoculated on the extraction medium and the number of cells was about 4×10⁵. The MTS cell viability assay was performed in at least 3 replicates of each measurement. After varying durations (1, 2 and 3 days) of cell culture, the medium in the well was discarded, the cells were washed with phosphate buffer saline (PBS), and the mixed solution (MTS: DMEM=1: 5) was added. The cells were cultured in an incubator with a constant temperature (37°C) for 1 h and then placed in 96-well plates filled with 200 μL of solution. The cell viability was evaluated by comparing the absorbance (OD) at 490 nm with Multiskan FC. By comparing the absorbance of the blank group and the test group, the cell viability rate was obtained to evaluate the biocompatibility of the hydrogels. L929 cells were stained using the calcein-AM/ETHD-I double staining assay after 3 days of culturing on the leaching medium for observation under an inverted fluorescence microscope.

Additional characterization

A scanning electron microscope (TM4000Plus II) was used to observe the morphologies of the hydrogels. Before the test, the hydrogels were freeze-dried to remove the water molecules while keeping its spatial structure intact. The samples were broken down in liquid nitrogen.














The experiments involving human subjects have been carried out with the full, informed consent of the volunteers, who are also co-authors of the paper.

Table S1 The mean and standard deviation values of elongation at break, strength, elastic modulus and work of fracture values of various fiber-based hydrogels.

Hydrogel	Elongation at break %	Strength MPa	Modulus MPa	Work of fracture MJ m⁻³
PF_5P	117±99	0.41±0.07	0.14±0.01	0.59±0.21
PF_10P	256±14	0.90±0.09	0.19±0.01	1.44±0.16
PF_15P	510±21	2.05±0.20	0.32±0.05	5.47±0.44
PF_20P	759±46	3.79±0.45	0.54±0.06	13.71±1.96
PF_10P10G	920±35	5.71±0.61	0.72±0.09	26.89±3.13
PF_10P30G	1126±92	9.20±0.47	1.49±0.14	54.07±4.91
PF_10P50G	1719±77	12.80±0.70	4.51±0.76	134.47±9.29

Table S2 Comparison of the mechanical properties of the hydrogels developed in our work with some other tough hydrogels

	Hydrogel	Elongation at break (%)	Strength (MPa)	Modulus (MPa)	Work of fracture (MJ m ⁻³)	Refs.	symbol
Our work	PF_10P50G	1767	14	5.3	145.5	-	★
	PF_10P50G (pre-stretching)	394	45	26.9	129.5	-	★
PVA based hydrogel	PVA/tC /Ca ²⁺	856	1.54	0.092	5.14	[5]	●
	PVA/ANFs/TA	950	2.06	-	-	[6]	○
	PVA/NaCl	730	8.03	1	28.7	[7]	◐
	PVA/ANF/ PANI	140	2.4	-	-	[8]	◑
	PVA/CNC/TA	1107.55	8.71	1.43	50.03	[9]	◒
	PVA/PHEA	2403	1.13	0.207	13.71	[10]	◓
	PVA/HA/PAA/PDA	988.76	11.76	-	-	[11]	⊕
	PVA/Agar/AS	544	18	7.5	42.3	[12]	⊗
	PVA/CS	406.4	4.02	2.07	9.31	[13]	⊖
	PVA/HA/Fe ³⁺	340	8	10	19.6	[14]	⊕
	polyacrylic acid-PVA	689	11.7	-	-	[15]	⊙
double network (DN) hydrogel	Zein/WPU	683	6.5	8.04	20.7	[16]	■
	PAA/GO-Fe ³⁺ /CS	600	2.75	0.82	8.5	[17]	□
	HAPAA/PANI	2590	0.9	-	7.85	[18]	▣
	P(AAc-co-Am)/PVA	1290	0.3295	-	-	[19]	▤
	CDs/HA/PVA	429	1.28	-	-	[20]	▥
	κ-CG/P(AAm-co-F127DA)	2000	1.11	-	10.83	[21]	▦
	PAMPS-PAAM	1096	2.24	-	-	[22]	▧
	PAMPS-PCDME	656	1.46	-	-	[23]	▨
B-DN gel membrane	942	8	-	-	[24]	▩	
glycerol-water (G-W) hydrogel	PVA/glycerol/NaCl	570.7	3.1	0.52	8.65	[25]	▲
	PVA/Gly/CB/CNT	643.2	4.8	1.001	15.93	[26]	△
	CPA	540	0.038	-	0.11	[27]	▴
	XG/PAAm	1769	1.5	0.32	11.91	[28]	▵
	PTCM-Gly	1500	0.16	-	-	[29]	▾
anisotropic hydrogel	PAM-AA/CNF/Fe ³⁺	480	11	-	-	[4]	▼

	ACHH	22.6	25.6	218.2	-	[30]	
	C ₄ (MO) ₃ N ₇ -16	135	5.48	23.5	-	[31]	
	CNFs/PAM	11	36	310	-	[32]	
	PMPTC/PNaSS	267.3±1.3	25.8±1.33	59.0±6.57	38.03±2.83	[33]	
other hydrogels	TPN	435	0.29			[34]	
	highly entangled	455	0.39			[35]	
	PAAm-PAA	350	3.27			[36]	
	HC-SI	340	3.5			[37]	
	PEDOT:PSS	17	2.14			[38]	
	PIC/AgNWs	645	3.3			[39]	
	PMPTC/PNaSS	750±80	5.1±0.6	7.9±0.6	18.8±1.9	[40]	
	PAAc/CaAc	77	15.44			[41]	
	PIC	210±54	6.8±0.85	56.3±12.5	10.4±2.4	[42]	

Note: The symbols in the table are corresponding to Figure 3d.

Table S3 Composition ratio of the impregnating solution

Hydrogel	Impregnating Solution	PVA (g)	Water (g)	Glycerin (g)	P/(W+G+P) (w/w %)	G/(W+G) (w/w %)
PF_5P	5% PVA	5	95	-	5	-
PF_10P	10% PVA	10	90	-	10	-
PF_15P	15% PVA	15	85	-	15	-
PF_20P	20% PVA	20	80	-	20	-
PF_10P10G	10% PVA (10% glycerin)	10	81	9	10	10
PF_10P30G	10% PVA (30% glycerin)	10	63	27	10	30
PF_10P50G	10% PVA (50% glycerin)	10	45	45	10	50

Note: P, G and W in the table are the abbreviations for PVA, glycerin and water, respectively.

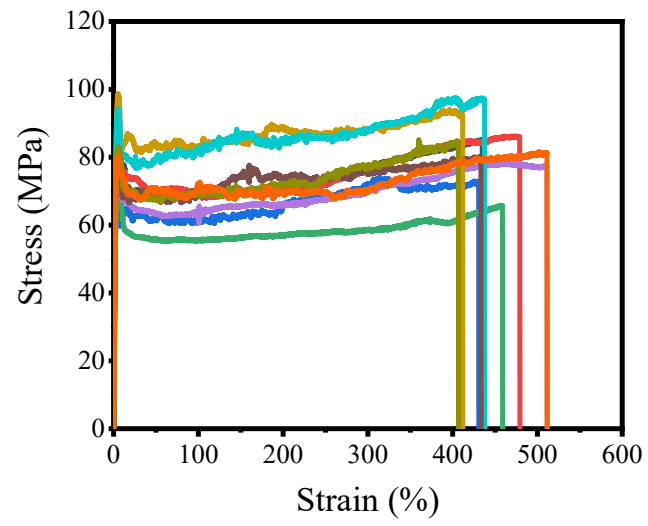


Figure S1 Tensile stress-strain curves of single PVA fiber (10 samples).

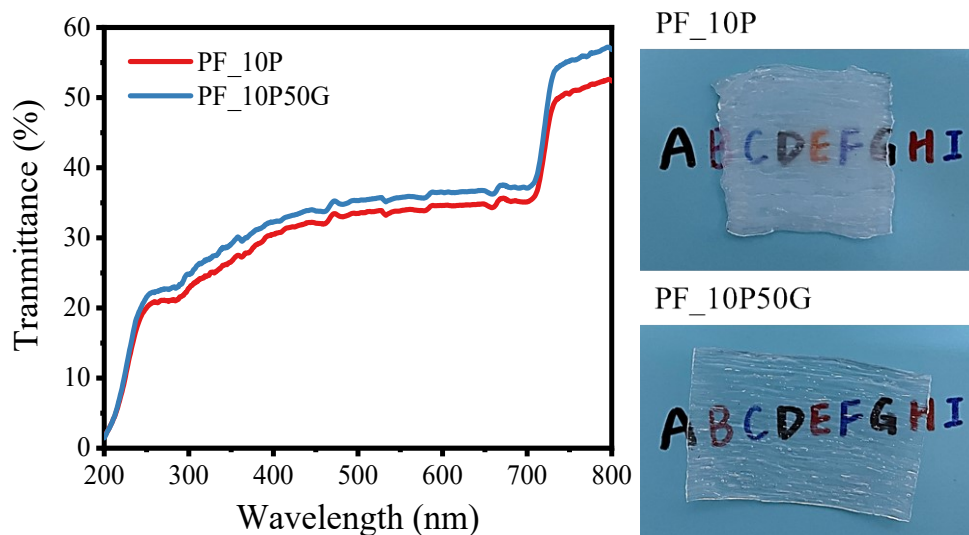


Figure S2 The transparency levels of PF_10P and PF_10P50G hydrogels.

The transmittance of the hydrogels was measured by an UV-visible infrared spectrophotometer (Shimadzu, UV-3600, Japan) in the wavelength range of 200-800 nm. PF_10P and PF_10P50G are translucent. Letters on the paper can be seen through the hydrogels, and PF_10P50G was clearer than PF_10P.

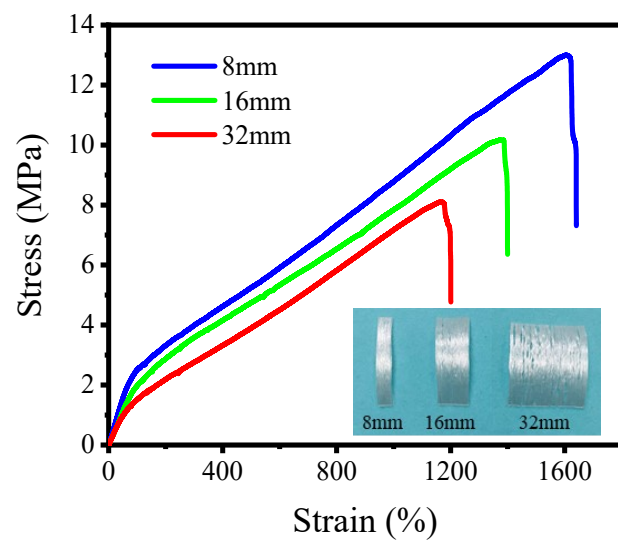


Figure S3 Tensile stress-strain curves of the PF_10P50G hydrogels with different widths.

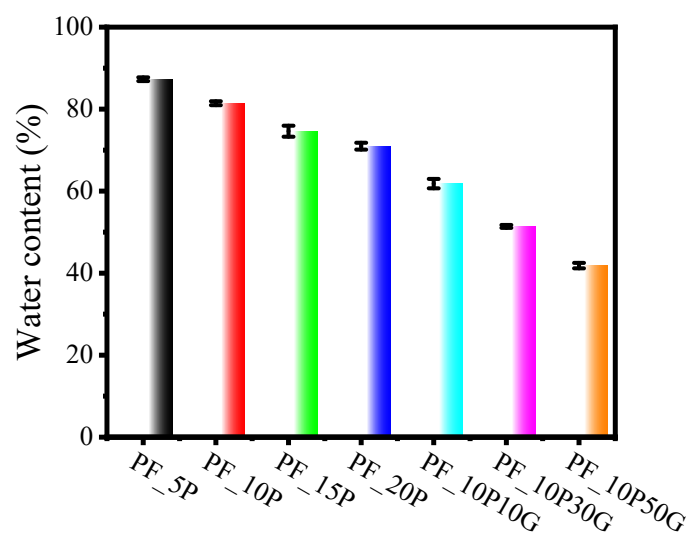


Figure S4 Water contents of various fiber-based hydrogels.

The water content (WC) was determined from the equation: $WC = (M_w - M_d) / M_d \times 100\%$, where M_w and M_d are the weight of anisotropic fibers-based hydrogels before and after freeze-drying. With the increase of the concentration of PVA and glycerol in the impregnating solution, the water content of hydrogel decreased gradually. The water content of PF_10P and PF_10P50G was $81.5 \pm 0.5\%$ and $41.8 \pm 0.7\%$, respectively. The decrease of the water content is because some water molecules in the hydrogel are replaced by glycerin, and glycerin will hinder the swelling of the PVA fiber, resulting in the decrease of fiber water absorption.

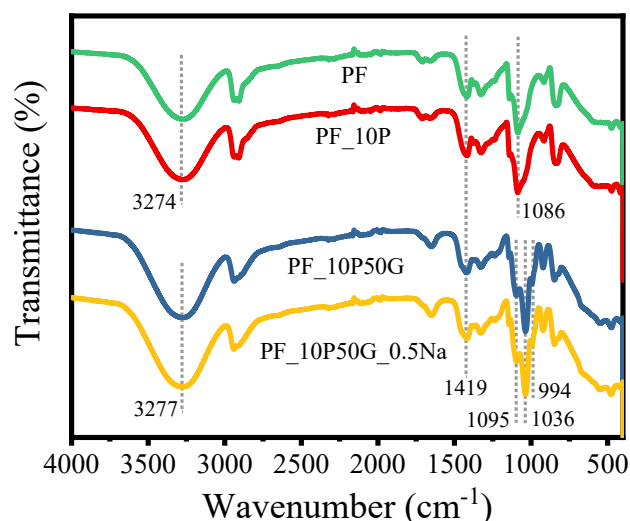


Figure S5 ATR-FTIR spectra of dried PVA fibers (PF), freeze-dried PF_10P, PF_10P50G and PF_10P50G_0.5Na hydrogels.

Attenuated total reflectance Fourier transform infrared spectroscopy (ATR-FTIR) of lyophilized hydrogels with different compositions was performed at room temperature by Nicolet iS50 to study the molecular structure and chemical bonds of the hydrogels.

In order to better understand the molecular interactions in hydrogels, we analyzed the total ATR-FTIR spectra of dried PVA fibers (PF), freeze-dried PF_10P, PF_10P50G and PF_10P50G_0.5Na hydrogels. Both PVA fibers and PF_10P are composed of PVA and have similar FTIR spectra, which show a broad characteristic peak at 3274 cm^{-1} for the O-H stretching vibrations, and peaks at 1419 and 1086 cm^{-1} for the CH_2 bending vibrations and C-O stretching vibrations.¹² Similarly, the PF_10P50G and PF_10P50G_0.5Na hydrogels are composed of PVA and glycerol and have similar FTIR spectra, which have a broad characteristic peak at 3277 cm^{-1} for the O-H stretching vibrations, and a peak at 1419 cm^{-1} for the CH_2 bending vibrations. The peak of asymmetric stretching vibrations for C-O is at 1095 cm^{-1} , while the peaks of symmetric stretching vibrations for C-O are at 1036 and 994 cm^{-1} , respectively.^{25, 43} The peak of stretching vibrations for O-H shifted from 3274 cm^{-1} to 3277 cm^{-1} when glycerol is added, indicating that glycerol forms hydrogen interaction with the PVA chain, which weakens the strong hydrogen bonds between PVA chain.⁴³ The hydrogen bonds between the PVA chains are broken, which densifies the hydrogels.⁴⁴

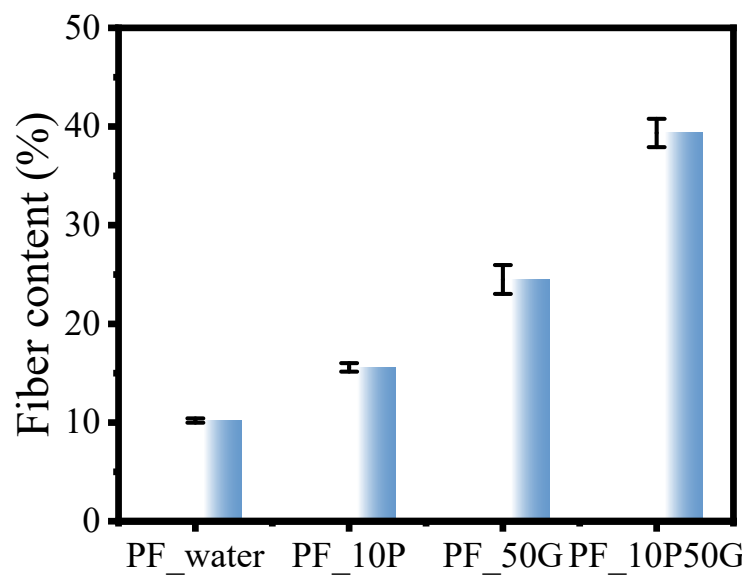


Figure S6 The mass fraction of fibers in PF_water, PF_10P, PF_50G, PF_10P50G hydrogels.

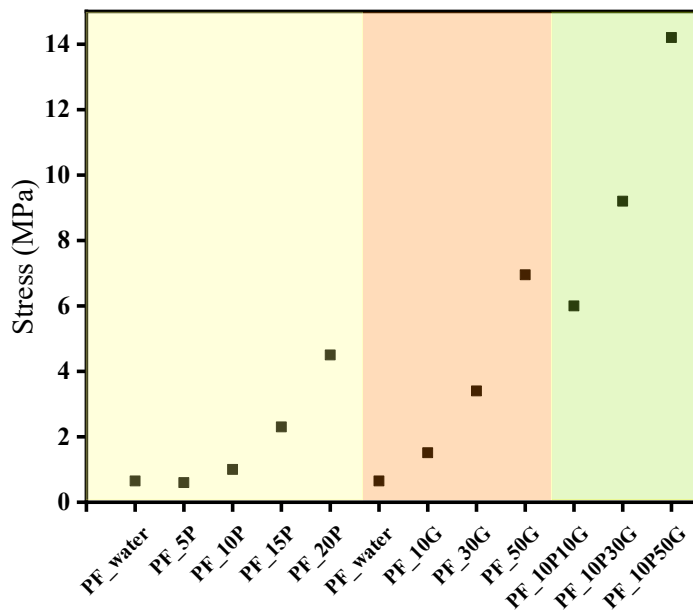


Figure S7 Stress of different hydrogels

Figure S5 demonstrated that the addition of glycerol results in the formation of hydrogen interaction with the PVA chain. Through the hydrogen interactions between glycerol and the PVA chain, the formation of multiple hydrogen bonds can occur.⁴⁵ With the increasing of glycerol content, the number of hydrogen bond also increases. These hydrogen bonds effectively crosslink the PVA chains and promote their binding, resulting in higher strength, modulus, and toughness of PF. In addition, references⁴⁶⁻⁴⁸ have reported that non-covalent interaction can reform the fractured bonds, thereby enabling partial or complete recovery. As a non-covalent bond, hydrogen bond (introduced by glycerol) can facilitate dynamic fracture and re-crosslinking, allowing the fractured bonds to reconnect. This also contributes to the improved mechanical properties especially the fracture resistance and toughness of PF. Moreover, glycerol is able to improve the effective crosslinking density of the hydrogels,⁴⁹ and the hydrogen bond zones can be utilized to achieve crack propagation insensitivity, effectively preventing the catastrophic propagation of fatigue cracks when fatigue damage occurs.

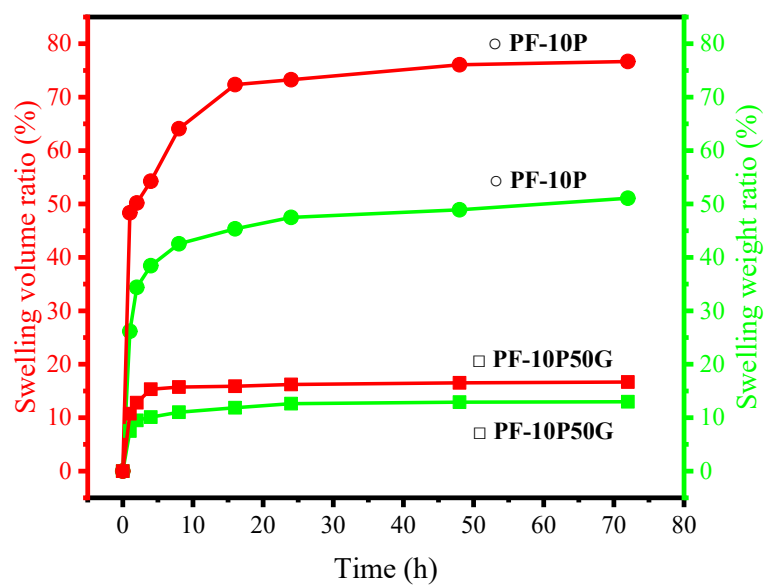


Figure S8 Swelling ratio of PF_10P and PF_10P50G hydrogels soaked in DI water for 72h

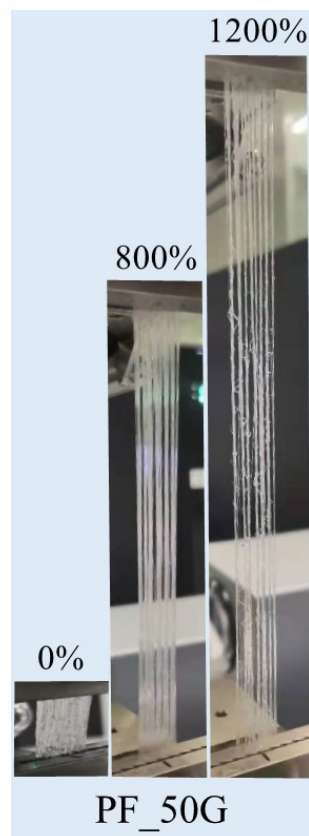
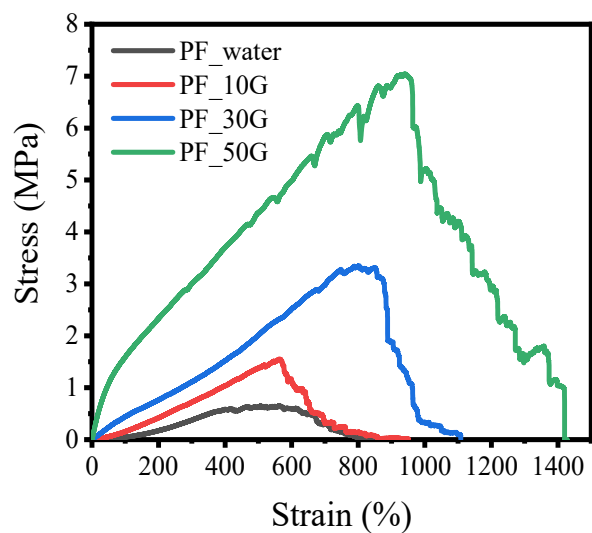


Figure S9 Tensile stress-strain curves of PF_water, PF_10G, PF_30G and PF_50G (The figure on the left). Tensile and fracture state of the PF_50G hydrogel (The figure on the right).

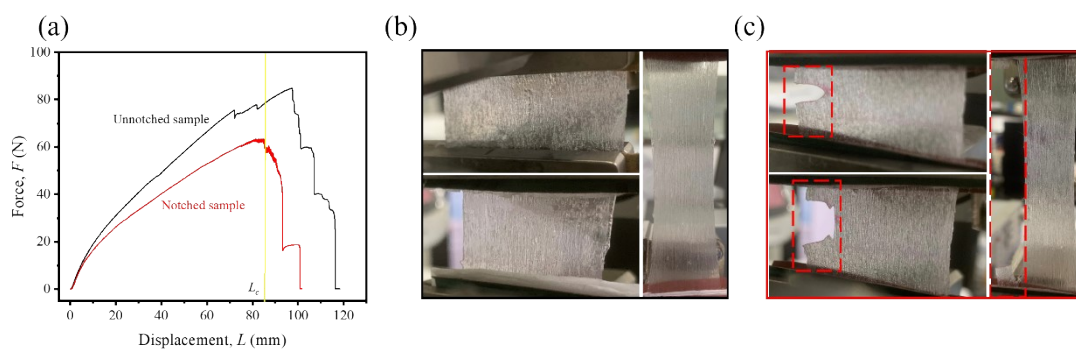


Figure S10 Force-extension curves of the unnotched and notched samples of PF-10P50G

To evaluate the fracture toughness of hydrogels, the classical pure shear test for measuring fracture energy of soft materials is performed. The fracture energy Γ calculated according to Figure S10 is 305.04 kJ m^{-2} , which contains both the energy for mechanical dissipation in regions around the crack due to viscoelasticity and the intrinsic fracture energy required to break polymer chains³. As shown in Figure S10, unique crack shape evolution and crack advance were observed during the pure shear test. As revealed by the images, the crack did not advance in the transverse direction. Therefore, this kind of materials shows high toughness.

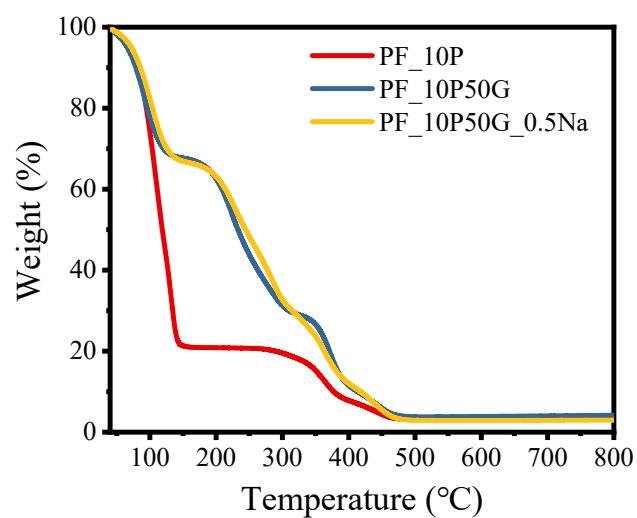


Figure S11 TGA curves of PF_10P, PF_10P50G and PF_10P50G_0.5Na hydrogels

The water retention capacity of hydrogels was further characterized by thermogravimetric analysis (TGA, Netzsch TG209). The temperature for testing increased from room temperature to 800°C at a scanning rate of 10°C min⁻¹ in N₂ atmosphere.

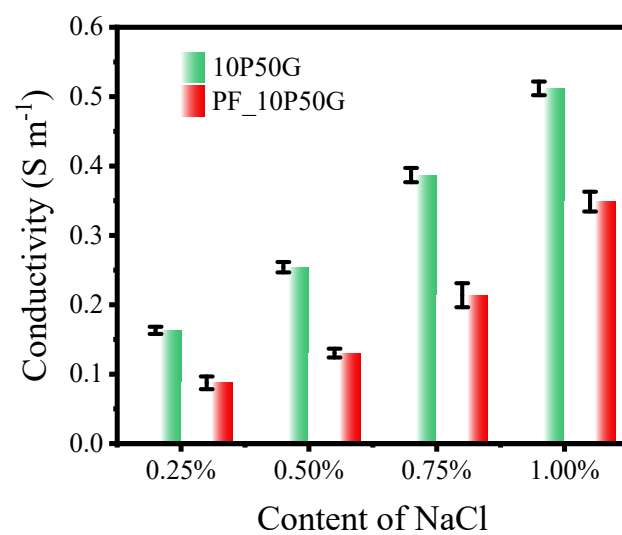


Figure S12 Ionic conductivity of 10P50G and PF_10P50G containing different contents of NaCl.

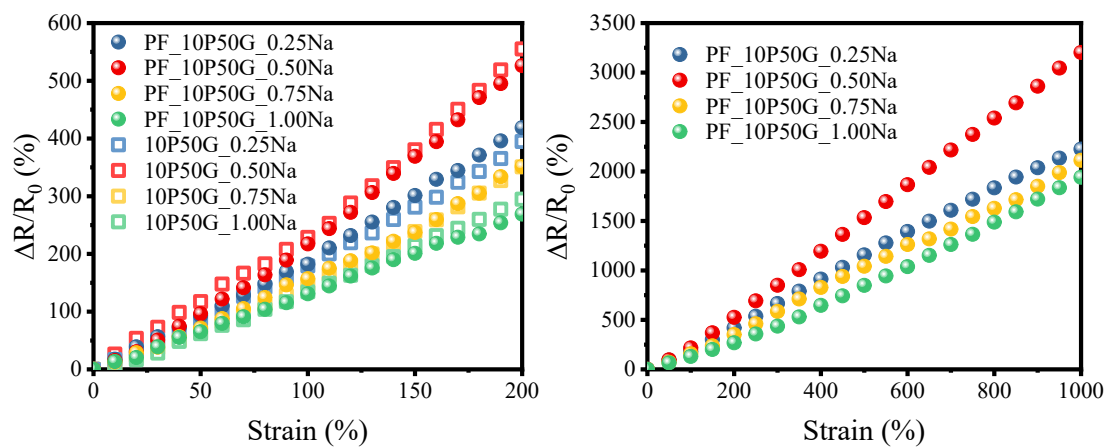


Figure S13 The relative resistance change rate-strain curves of PF_10P50G_Na (strain=1000%) and 10P50G_Na (strain=200%).

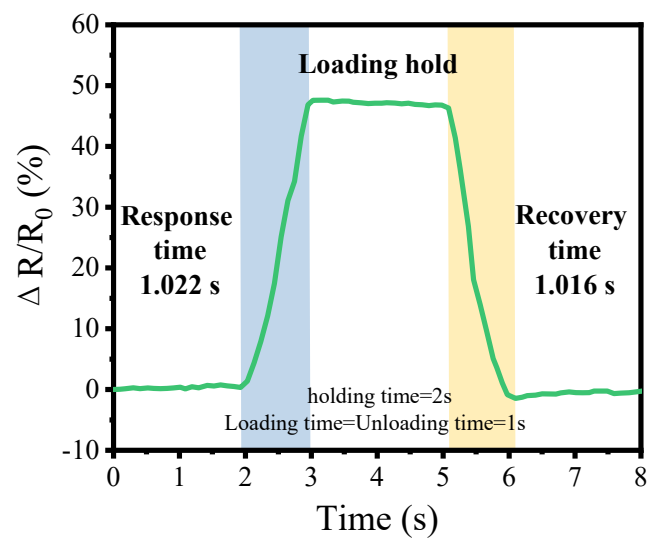


Figure S14 Response and recovery time of the PF_10P50G_0.5Na hydrogel (strain=30%).

References

1. Jalal Uddin, A.; Araki, J.; Gotoh, Y., Toward "strong" green nanocomposites: polyvinyl alcohol reinforced with extremely oriented cellulose whiskers. *Biomacromolecules* **2011**, *12* (3), 617-24.
2. Peng, J.; Ellingham, T.; Sabo, R.; Turng, L.-S.; Clemons, C. M., Short cellulose nanofibrils as reinforcement in polyvinyl alcohol fiber. *Cellulose* **2014**, *21* (6), 4287-4298.
3. Luo, F.; Sun, T. L.; Nakajima, T.; Kurokawa, T.; Zhao, Y.; Ihsan, A. B.; Guo, H. L.; Li, X. F.; Gong, J. P., Crack blunting and advancing behaviors of tough and self-healing polyampholyte hydrogel. *Macromolecules* **2014**, *47* (17), 6037-6046.
4. Geng, L.; Hu, S.; Cui, M.; Wu, J.; Huang, A.; Shi, S.; Peng, X., Muscle-inspired double-network hydrogels with robust mechanical property, biocompatibility and ionic conductivity. *Carbohydr Polym* **2021**, *262*, 117936.
5. Jing, H.; Shi, J.; Guoab, P.; Guan, S.; Fu, H.; Cui, W., Hydrogels based on physically cross-linked network with high mechanical property and recasting ability. *Colloids and Surfaces A: Physicochemical and Engineering Aspects* **2021**, *611*.
6. Guo, Y.; An, X.; Fan, Z., Aramid nanofibers reinforced polyvinyl alcohol/tannic acid hydrogel with improved mechanical and antibacterial properties for potential application as wound dressing. *J Mech Behav Biomed Mater* **2021**, *118*, 104452.
7. Di, X.; Ma, Q.; Xu, Y.; Yang, M.; Wu, G.; Sun, P., High-performance ionic conductive poly(vinyl alcohol) hydrogels for flexible strain sensors based on a universal soaking strategy. *Materials Chemistry Frontiers* **2021**, *5* (1), 315-323.
8. Wang, J.; Lin, Y.; Mohamed, A.; Ji, Q.; Jia, H., High strength and flexible aramid nanofiber conductive hydrogels for wearable strain sensors. *Journal of Materials Chemistry C* **2021**, *9* (2), 575-583.
9. Lin, F.; Wang, Z.; Chen, J.; Lu, B.; Tang, L.; Chen, X.; Lin, C.; Huang, B.; Zeng, H.; Chen, Y., A bioinspired hydrogen bond crosslink strategy toward toughening ultrastrong and multifunctional nanocomposite hydrogels. *J Mater Chem B* **2020**, *8* (18), 4002-4015.
10. Yang, J.; Yu, X.; Sun, X.; Kang, Q.; Zhu, L.; Qin, G.; Zhou, A.; Sun, G.; Chen, Q., Polyaniline-Decorated Supramolecular Hydrogel with Tough, Fatigue-Resistant, and Self-Healable Performances for All-In-One Flexible Supercapacitors. *ACS Appl Mater Interfaces* **2020**, *12* (8), 9736-9745.
11. Chen, K.; Liu, S.; Wu, X.; Wang, F.; Chen, G.; Yang, X.; Xu, L.; Qi, J.; Luo, Y.; Zhang, D., Mussel-inspired construction of Ti6Al4V-hydrogel artificial cartilage material with high strength and low friction. *Materials Letters* **2020**, *265*.
12. Sun, X.; Luo, C.; Luo, F., Preparation and properties of self-healable and conductive PVA-agar hydrogel with ultra-high mechanical strength. *European Polymer Journal* **2020**, *124*.
13. Xiang, X.; Chen, G.; Chen, K.; Jiang, X.; Hou, L., Facile preparation and characterization of super tough chitosan/poly(vinyl alcohol) hydrogel with low temperature resistance and anti-swelling property. *Int J Biol Macromol* **2020**, *142*, 574-582.
14. Li, A.; Si, Y.; Wang, X.; Jia, X.; Guo, X.; Xu, Y., Poly(vinyl alcohol) Nanocrystal-Assisted Hydrogels with High Toughness and Elastic Modulus for Three-Dimensional Printing. *ACS Applied Nano Materials* **2019**, *2* (2), 707-715.
15. Liu, X.; Steiger, C.; Lin, S.; Parada, G. A.; Liu, J.; Chan, H. F.; Yuk, H.; Phan, N. V.; Collins, J.; Tamang, S.; Traverso, G.; Zhao, X., Ingestible hydrogel device. *Nat Commun* **2019**, *10* (1), 493.
16. Lu, X.; Cao, L.; Yin, X.; Si, Y.; Yu, J.; Ding, B., Stretchable, tough and elastic nanofibrous hydrogels with dermis-mimicking network structure. *J Colloid Interface Sci* **2021**, *582* (Pt A), 387-395.

17. Zhang, Y.; Li, M.; Han, X.; Fan, Z.; Zhang, H.; Li, Q., High-strength and highly electrically conductive hydrogels for wearable strain sensor. *Chemical Physics Letters* **2021**, 769.
18. Su, G.; Yin, S.; Guo, Y.; Zhao, F.; Guo, Q.; Zhang, X.; Zhou, T.; Yu, G., Balancing the mechanical, electronic, and self-healing properties in conductive self-healing hydrogel for wearable sensor applications. *Materials Horizons* **2021**, 8 (6), 1795-1804.
19. Jing, Z.; Xu, A.; Liang, Y. Q.; Zhang, Z.; Yu, C.; Hong, P.; Li, Y., Biodegradable Poly(acrylic acid-co-acrylamide)/Poly(vinyl alcohol) Double Network Hydrogels with Tunable Mechanics and High Self-healing Performance. *Polymers (Basel)* **2019**, 11 (6).
20. Wang, Y.; Xue, Y.; Wang, J.; Zhu, Y.; Zhu, Y.; Zhang, X.; Liao, J.; Li, X.; Wu, X.; Qin, Y. X.; Chen, W., A Composite Hydrogel with High Mechanical Strength, Fluorescence, and Degradable Behavior for Bone Tissue Engineering. *Polymers (Basel)* **2019**, 11 (7).
21. Zhou, L.; Pei, X.; Fang, K.; Zhang, R.; Fu, J., Super tough, ultra-stretchable, and fast recoverable double network hydrogels physically crosslinked by triple non-covalent interactions. *Polymer* **2020**, 192.
22. Wang, Y.; Liang, D.; Suo, Z.; Jia, K., Synergy of noncovalent interlink and covalent toughener for tough hydrogel adhesion. *Extreme Mechanics Letters* **2020**, 39.
23. Yin, H.; King, D. R.; Sun, T. L.; Saruwatari, Y.; Nakajima, T.; Kurokawa, T.; Gong, J. P., Polyzwitterions as a Versatile Building Block of Tough Hydrogels: From Polyelectrolyte Complex Gels to Double-Network Gels. *ACS Appl Mater Interfaces* **2020**, 12 (44), 50068-50076.
24. Ye, Y. N.; Frauenlob, M.; Wang, L.; Tsuda, M.; Sun, T. L.; Cui, K.; Takahashi, R.; Zhang, H. J.; Nakajima, T.; Nonoyama, T.; Kurokawa, T.; Tanaka, S.; Gong, J. P., Tough and Self-Recoverable Thin Hydrogel Membranes for Biological Applications. *Advanced Functional Materials* **2018**, 28 (31).
25. Pan, S.; Xia, M.; Li, H.; Jiang, X.; He, P.; Sun, Z.; Zhang, Y., Transparent, high-strength, stretchable, sensitive and anti-freezing poly(vinyl alcohol) ionic hydrogel strain sensors for human motion monitoring. *Journal of Materials Chemistry C* **2020**, 8 (8), 2827-2837.
26. Gu, J.; Huang, J.; Chen, G.; Hou, L.; Zhang, J.; Zhang, X.; Yang, X.; Guan, L.; Jiang, X.; Liu, H., Multifunctional Poly(vinyl alcohol) Nanocomposite Organohydrogel for Flexible Strain and Temperature Sensor. *ACS Appl Mater Interfaces* **2020**, 12 (36), 40815-40827.
27. You, Z.; Dong, Y.; Li, X.; Yang, P.; Luo, M.; Zhu, Z.; Wu, L.; Zhou, X.; Chen, M., One-pot synthesis of multi-functional cellulose-based ionic conductive organohydrogel with low-temperature strain sensitivity. *Carbohydr Polym* **2021**, 251, 117019.
28. Yu, Q.; Qin, Z.; Ji, F.; Chen, S.; Luo, S.; Yao, M.; Wu, X.; Liu, W.; Sun, X.; Zhang, H.; Zhao, Y.; Yao, F.; Li, J., Low-temperature tolerant strain sensors based on triple crosslinked organohydrogels with ultrastretchability. *Chemical Engineering Journal* **2021**, 404.
29. Wei, Y.; Xiang, L.; Ou, H.; Li, F.; Zhang, Y.; Qian, Y.; Hao, L.; Diao, J.; Zhang, M.; Zhu, P.; Liu, Y.; Kuang, Y.; Chen, G., MXene-Based Conductive Organohydrogels with Long-Term Environmental Stability and Multifunctionality. *Advanced Functional Materials* **2020**, 30 (48).
30. Wang, Y.; Liu, S.; Yu, W., Bioinspired Anisotropic Chitosan Hybrid Hydrogel. *ACS Applied Bio Materials* **2020**, 3 (10), 6959-6966.
31. Wei, P.; Chen, T.; Chen, G.; Hou, K.; Zhu, M., Ligament-Inspired Tough and Anisotropic Fibrous Gel Belt with Programed Shape Deformations via Dynamic Stretching. *ACS Appl Mater Interfaces* **2021**, 13 (16), 19291-19300.
32. Kong, W.; Wang, C.; Jia, C.; Kuang, Y.; Pastel, G.; Chen, C.; Chen, G.; He, S.; Huang, H.; Zhang, J.; Wang, S.; Hu, L., Muscle-Inspired Highly Anisotropic, Strong, Ion-Conductive Hydrogels. *Adv Mater* **2018**, 30 (39), e1801934.

33. Mredha, M. T. I.; Guo, Y. Z.; Nonoyama, T.; Nakajima, T.; Kurokawa, T.; Gong, J. P., A Facile Method to Fabricate Anisotropic Hydrogels with Perfectly Aligned Hierarchical Fibrous Structures. *Adv Mater* **2018**, *30* (9).
34. Liu, X.; Wu, J.; Qiao, K.; Liu, G.; Wang, Z.; Lu, T.; Suo, Z.; Hu, J., Topoarchitected polymer networks expand the space of material properties. *Nat Commun* **2022**, *13* (1), 1622.
35. Kim, J.; Zhang, G. G.; Shi, M. X.; Suo, Z. G., Fracture, fatigue, and friction of polymers in which entanglements greatly outnumber cross-links. *Science* **2021**, *374* (6564), 212-+.
36. Yang, H.; Ji, M.; Yang, M.; Shi, M.; Pan, Y.; Zhou, Y.; Qi, H. J.; Suo, Z.; Tang, J., Fabricating hydrogels to mimic biological tissues of complex shapes and high fatigue resistance. *Matter* **2021**, *4* (6), 1935-1946.
37. Ni, J.; Lin, S.; Qin, Z.; Veysset, D.; Liu, X.; Sun, Y.; Hsieh, A. J.; Radovitzky, R.; Nelson, K. A.; Zhao, X., Strong fatigue-resistant nanofibrous hydrogels inspired by lobster underbelly. *Matter* **2021**, *4* (6), 1919-1934.
38. Lu, B.; Yuk, H.; Lin, S.; Jian, N.; Qu, K.; Xu, J.; Zhao, X., Pure PEDOT:PSS hydrogels. *Nat Commun* **2019**, *10* (1), 1043.
39. Zhu, F.; Zheng, S. Y.; Lin, J.; Wu, Z. L.; Yin, J.; Qian, J.; Qu, S.; Zheng, Q., Integrated multifunctional flexible electronics based on tough supramolecular hydrogels with patterned silver nanowires. *Journal of Materials Chemistry C* **2020**, *8* (23), 7688-7697.
40. Luo, F.; Sun, T. L.; Nakajima, T.; Kurokawa, T.; Zhao, Y.; Sato, K.; Ihsan, A. B.; Li, X.; Guo, H.; Gong, J. P., Oppositely charged polyelectrolytes form tough, self-healing, and rebuildable hydrogels. *Adv Mater* **2015**, *27* (17), 2722-7.
41. Nonoyama, T.; Lee, Y. W.; Ota, K.; Fujioka, K.; Hong, W.; Gong, J. P., Instant Thermal Switching from Soft Hydrogel to Rigid Plastics Inspired by Thermophile Proteins. *Adv Mater* **2020**, *32* (4), e1905878.
42. Luo, F.; Sun, T. L.; Nakajima, T.; Kurokawa, T.; Li, X.; Guo, H.; Huang, Y.; Zhang, H.; Gong, J. P., Tough polyion-complex hydrogels from soft to stiff controlled by monomer structure. *Polymer* **2017**, *116*, 487-497.
43. Peng, S.; Liu, S.; Sun, Y.; Xiang, N.; Jiang, X.; Hou, L., Facile preparation and characterization of poly(vinyl alcohol)-NaCl-glycerol supramolecular hydrogel electrolyte. *European Polymer Journal* **2018**, *106*, 206-213.
44. Chen, W.; Li, N.; Ma, Y.; Minus, M. L.; Benson, K.; Lu, X.; Wang, X.; Ling, X.; Zhu, H., Superstrong and Tough Hydrogel through Physical Cross-Linking and Molecular Alignment. *Biomacromolecules* **2019**, *20* (12), 4476-4484.
45. Shi, S.; Peng, X.; Liu, T.; Chen, Y.-N.; He, C.; Wang, H., Facile preparation of hydrogen-bonded supramolecular polyvinyl alcohol-glycerol gels with excellent thermoplasticity and mechanical properties. *Polymer* **2017**, *111*, 168-176.
46. Henderson, K. J.; Zhou, T. C.; Otim, K. J.; Shull, K. R., Ionically cross-linked triblock copolymer hydrogels with high strength. *Macromolecules* **2010**, *43* (14), 6193-6201.
47. Haque, M. A.; Kurokawa, T.; Kamita, G.; Gong, J. P., Lamellar bilayers as reversible sacrificial bonds to toughen hydrogel: hysteresis, self-recovery, fatigue resistance, and crack blunting. *Macromolecules* **2011**, *44* (22), 8916-8924.
48. Sun, J.-Y.; Zhao, X.; Illeperuma, W. R.; Chaudhuri, O.; Oh, K. H.; Mooney, D. J.; Vlassak, J. J.; Suo, Z., Highly stretchable and tough hydrogels. *Nature* **2012**, *489* (7414), 133-136.
49. Zhu, X.; Zhang, Y.; Deng, J.; Luo, X., Effect of Glycerol on the Properties of the Cross-Linked Polyvinyl Alcohol Hydrogel Beads. *ChemistrySelect* **2018**, *3* (2), 467-470.
50. Li, W.; Wang, X.; Liu, Z.; Zou, X.; Shen, Z.; Liu, D.; Li, L.; Guo, Y.; Yan, F.,

Nanoconfined polymerization limits crack propagation in hysteresis-free gels. *Nature Materials* **2023**, 1-8.